Clays and Clay Minerals, Vol. 40, No. 4, 369–380, 1992.

STRUCTURAL CHARACTERISATION OF KAOLINITE:NaCl INTERCALATE AND ITS DERIVATIVES

JOHN G. THOMPSON,[1,4] PHILIPPA J. R. UWINS,[2] ANDREW K. WHITTAKER,[3] AND IAN D. R. MACKINNON[2]

[1] Research School of Chemistry, Australian National University, GPO Box 4, Canberra, ACT 2601, Australia

[2] Centre for Microscopy and Microanalysis, University of Queensland, QLD 4072, Australia

[3] Centre for Magnetic Resonance, University of Queensland, QLD 4072, Australia

Abstract—Kaolinite:NaCl intercalates with basal layer dimensions of 0.95 and 1.25 nm have been prepared by direct reaction of saturated aqueous NaCl solution with well-crystallized source clay KGa-1. The intercalates and their thermal decomposition products have been studied by XRD, solid-state ^{23}Na, ^{27}Al, and ^{29}Si MAS NMR, and FTIR. Intercalate yield is enhanced by dry grinding of kaolinite with NaCl prior to intercalation. The layered structure survives dehydroxylation of the kaolinite at 500°–600°C and persists to above 800°C with a resultant tetrahedral aluminosilicate framework. Excess NaCl can be readily removed by rinsing with water, producing an XRD 'amorphous' material. Upon heating at 900°C this material converts to a well-crystallized framework aluminosilicate closely related to low-carnegieite, $NaAlSiO_4$, some 350°C below its stability field. Reaction mechanisms are discussed and structural models proposed for each of these novel materials.

Key Words—FTIR, Intercalate, Kaolinite, NaCl, NMR, Structure, Synthesis, XRD.

INTRODUCTION

The seminal work on kaolinite intercalates by Weiss *et al.* (1966) showed that almost all types of alkali halides could be introduced into the kaolinite interlayer by the use of an entraining agent such as ammonium acetate. Since this work there has not been any further direct investigation of kaolinite alkali halide intercalates. However, Miller and Oulton (1972) almost certainly observed the formation of kaolinite:KBr intercalate in their infrared spectroscopic study of the effects of severe grinding of kaolinite with KBr. More recently direct reaction of CsCl with kaolinite has been used to produce a reactive intermediate in the quantitative formation of kaolinite:dimethylsulfoxide (DMSO) intercalate (Jackson and Abdel-Kader, 1978; Calvert, 1984), used for discriminating kaolin-group minerals via X-ray powder diffraction (XRD) from other minerals, e.g., chlorites, displaying XRD peaks at ~0.72 nm. The only reported study of the interaction of alkali halide solutions with kaolinite as a function of temperature, 25° to 1300°C (Gábor *et al.*, 1989), gave no clear indication that intercalation compounds had been synthesized.

Successful intercalation of kaolinite is commonly gauged by expansion of the basal layer dimension from approximately 0.72 nm to between 1.0 nm and 1.5 nm, depending on the nature of the intercalant. Thus, the intercalation reaction is readily monitored by the use of conventional powder X-ray diffraction (XRD) techniques. The degree of success, or the yield of the intercalation reaction, is calculated from the relative intensities of intercalated and un-intercalated basal spacings, respectively. Other methods for solid-state characterisation, such as infra-red (IR) and nuclear magnetic resonance (NMR) spectroscopy, are also used to monitor the progress of an intercalation reaction and to determine site-specific chemistry of intermediates and products. In this study of kaolinite:alkali halide intercalation, we employ XRD, FTIR, solid-state NMR, and electron microscopy to document the intercalation reaction and to determine relative stabilities of the resultant phase(s).

In general, studies on kaolinite intercalates show that (1) the intercalation reaction can occur at low temperatures, (2) the intercalation reaction is generally reversible, and (3) the stability of intercalated kaolinite products is also variable. For example, kaolinites readily intercalate with hydrazine at room temperature but equally readily decompose in the absence of excess hydrazine (Weiss *et al.*, 1966); whereas, kaolinite:DMSO is stable in air at temperatures in excess of 100°C (Thompson and Cuff, 1985). A transmission electron microscope (TEM) study of kaolinite:CsBr showed that the intercalate could tolerate localized electron beam heating similar to kaolinite (J. G. Thompson, personal communication). Recent work by Sugahara *et al.* (1988, 1990) on the *in situ* polymerization of the polar monomers acrylonitrile and acrylamide in the interlayer has produced kaolinite polyacrylonitrile and polyacrylamide intercalates which are stable to 300°C. A notable property of most kaolinite intercalates, except the polymer intercalates, is the ready reversibility of intercalation in the presence of excess water.

[4] Author to whom correspondence should be addressed.

Clearly, the utility of kaolinite intercalates in industrial processes, environmental decontamination or biomedical applications depends to a large degree upon the ease of formation, thermal stability, and the quality, or yield, of the final product. In this study, we present a systematic approach to the production of kaolinite:alkali halide intercalates which have good thermal stability to at least 800°C. In addition, the thermal decomposition products of kaolinite:NaCl intercalate show properties which suggest new, kinetically favourable pathways for the synthesis of aluminosilicate structures with novel tetrahedral configurations.

EXPERIMENTAL

Materials

Well known and analytically pure starting materials were used for all synthesis experiments. The Georgia kaolinite source clay (KGa-1; well-crystallized) and A. R. grade NaCl were used in the synthesis of the kaolinite:NaCl intercalate. In addition the synthetic low-carnegieite $NaAlSiO_4$ was made via conventional solid-state techniques (Klingenberg *et al.*, 1981) using 99.9% pure SiO_2 and Al_2O_3 and A. R. grade Na_2CO_3.

Synthesis

The synthesis of the kaolinite:NaCl intercalate and its subsequent decomposition products is divided into four steps:

Step 1. Initial reaction with NaCl (intercalation step)
Dry grind the clay with an excess of NaCl in a mortar with a pestle for a minimum of 5 minutes. This was followed by dispersing the clay/salt mixture in sufficient distilled water to make a saturated NaCl solution (~7 M at 298 K) then heating to dryness on a hot plate. This step was repeated if the intercalation reaction did not proceed to >95%.

Step 2. Heating the intercalate
Specimen containing >95% intercalated kaolinite, still in the presence of the excess NaCl, was heated in a muffle furnace at 200° to 1000°C in steps of 100° or 150°C for times ranging from 5 minutes to several hours.

Step 3. Rinsing to remove excess NaCl
The thermally treated specimen was dispersed thoroughly in distilled water then centrifuged to reclaim the reaction product. This step was repeated (typically 5 times) until no further chloride ions were detectable in the elute by the addition of silver nitrate solution. Excess water was removed from specimens both at room temperature under vacuum (10^{-6} torr) or by heating overnight at 105°C.

Step 4. Second heating
The rinsed/dried material was fired overnight at 900°C.

Characterization

The course of reaction and the reaction products were studied by various complementary spectroscopic, diffraction, and electron beam techniques. These are described below.

1) X-ray powder diffraction (XRD) patterns were collected on a Philips X-ray powder diffractometer using Ni-filtered CuKα with a Sietronics Sie112m automated stepping motor control upgrade.
2) Fourier transform infrared (FTIR) spectra from 400 to 4000 cm^{-1} were collected using a Perkins Elmer 1800 Fourier Transform Infrared Spectrophotometer. Specimens were very lightly ground with dry KBr powder before being pressed into pellets.
3) NMR results were obtained on a Bruker MSL300 spectrometer operating at 59.627 MHz, 78.205 MHz, and 79.390 MHz for ^{29}Si, ^{27}Al, and ^{23}Na, respectively. Samples were spun at the magic angle at 5 kHz (^{29}Si) or at 10 kHz (^{27}Al and ^{23}Na) in Bruker double air bearing probes. ^{29}Si spectra were collected using cross-polarisation or the single pulse excitation technique. The $\pi/2$ pulse time for ^{1}H and ^{29}Si was 3.7 s. For the cross-polarisation spectra, a contact time of 5 ms and a recycle delay of 3 s were used. ^{27}Al spectra were obtained using the single pulse excitation technique with an rf pulse time of 1 s. We used a pulse recycle delay of 1 s for these experiments. ^{23}Na spectra were recorded using the single pulse excitation technique with an rf pulse width of 1.5 s. A recycle delay of up to 4 s was necessary for full relaxation of the ^{23}Na spins.
4) Scanning electron microscopy (SEM) was performed with Jeol 890F and Jeol 6400F scanning electron microscopes, the latter equipped with a Link Si EDS and Moran Scientific Analyser. Samples were analysed in the SEM without a conductive metal or carbon coating.
5) Transmission electron microscopy (TEM) was performed on samples dispersed on holey carbon films using a Jeol 4000FX instrument. In some instances, we used a Gatan liquid nitrogen cooled, double-tilt cold stage for TEM analysis.

RESULTS

XRD

The kaolinite reacted with the saturated NaCl solution under the conditions described above (Step 1) to give a NaCl intercalate. Heating untreated kaolinite with saturated NaCl solution (~7 M) on a hot plate to dryness (i.e., >100°C) produced approximately 50–80% yield of intercalate. However, thoroughly dry grinding the kaolinite with NaCl before reaction improved the yield to ~90% using the hot plate. As dry grinding of kaolinite with alkali halide is known to introduce stacking and other disorder, we surmised that such disorder

in the starting material enhances the yield. We estimated the intercalate yield from the reduction in size of the integrated 0.72 nm peak relative to the starting kaolinite/NaCl mixture before heating.

The XRD profiles indicated the formation of an intercalate with a mixture of basal dimensions—0.125 nm and 0.95 nm. Figure 1 shows the XRD profile of the starting KGa-1 kaolinite (a) juxtaposed to that of the product of Step 1 (b). The remnant 0.72 nm peak in Figure 1b corresponds to ~5% of unintercalated material. The presence of this unintercalated material proved useful in monitoring the progress of reaction in Step 2. That the 1.25 nm and 0.95 nm peaks are basal reflections is verified by the observation that these peaks display the same preferred orientation behaviour as the 0.72 nm peak of the unintercalated material. This is also consistent with earlier unpublished TEM direct observation of ~1.1 nm basal spacings in kaolinite:CsBr intercalate (J. G. Thompson, personal communication). While such direct observations by TEM on kaolinite:NaCl have not yet been achieved, both TEM and SEM confirm that there is no noticeable change in crystal morphology. This would not be so if there were major reconstruction of the crystal lattice.

Rinsing this intercalate with water removes all the NaCl and the basal dimension returns to 0.72 nm. The XRD profile of the thoroughly rinsed material is shown in Figure 1c. This result confirms that Step 1 does not involve any reconstruction of the lattice (apart from the breaking of weak hydrogen bonds) and is thus completely reversible, except that the collapsed material is now very disordered as evident from the 02*l*, 11*l* region of the diffraction profile (i.e., 19 to 24° 2θ).

Heating the above material for between 20 and 60 minutes at ~800°C (Step 2) causes the unintercalated kaolinite to thoroughly dehydroxylate. Figure 2 shows the XRD profiles of a ~95% intercalated specimen heated for 30–60 minutes at progressively higher temperatures. Dehydroxylation of unintercalated kaolinite, which occurs at between 500 and 600°C, is known to cause the disappearance of the 0.72 nm and all of the other kaolinite peaks with the corresponding growth of a broad 'hump' between 0.45 and 0.30 nm (19 and 30° 2θ). In the XRD profile of the 800°C treated intercalate (Figure 3a), the 0.72 nm peak corresponding to the ~5% unintercalated material disappears, yet there is no noticeable broad 'hump' between 0.45 and 0.30 nm as observed when kaolinite dehydroxylates to form meta-kaolinite. Instead the 1.25 nm and 0.95 nm peaks persist, a weak broad feature between 0.70 and 0.55 nm (12 and 16° 2θ) appears, and a somewhat more intense broad feature centred on 0.27 nm (33° 2θ) (under the NaCl 200 reflection) also appears. Intense sharp peaks due to NaCl tend to dominate the XRD profile. It should be noted that heating the material for much longer than a few hours above ~700°C results in the formation of sodalite, $Na_4Al_3Si_3O_{12}Cl$ (XRD profile not shown). This is not unexpected as the reaction of kaolinite with NaCl to form sodalite has been known for some time (Deer *et al.*, 1966).

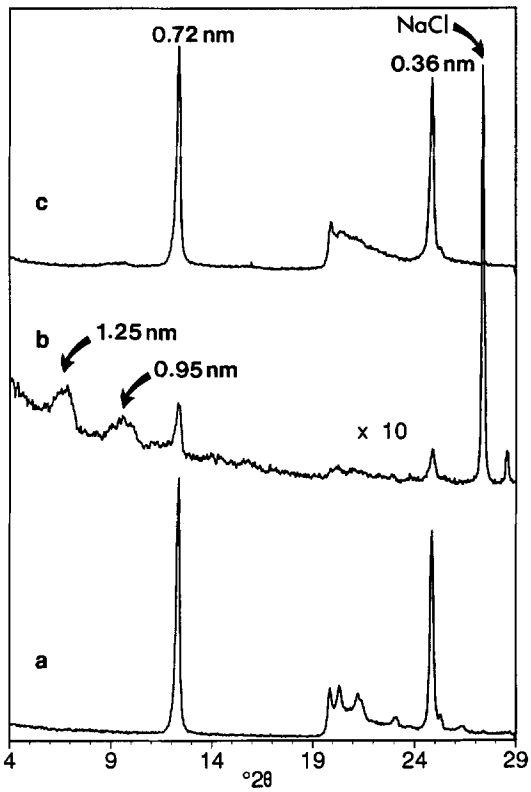

Figure 1. XRD profile (CuKα 4–29° 2θ) of well-crystallized KGa-1 (a) juxtaposed to the product of Step 1 and (b) vertical scale ×10 with respect to the other profiles. The broad peaks at low angle in (b) correspond to 1.25 and 0.95 nm kaolinite:NaCl intercalates basal reflections. The remnant 0.72 nm peak in (b) corresponds to ~5% of unintercalated material. Rinsing this material with water removes all the NaCl and the basal dimension returns to 0.72 nm (c).

The product of Step 2 was repeatedly rinsed with distilled water to remove any excess NaCl or Cl^- (Step 3), then dried either under vacuum at RT or in an oven at 105°C overnight. $AgNO_3$ solution was added to the elute to monitor the success of this process and 5 rinses appeared adequate. The elute showed no perceptible acidity suggesting that the HCl had disappeared during Step 2. The XRD profile (Figure 3b) shows the disappearance of the 1.25 nm and 0.95 nm peaks and the emergence of a sizeable, very broad hump between ~0.50 and 0.25 nm (18 and 36° 2θ). Apart from peaks due to $Al_4Ti_2SiO_{12}$ (labelled Ti-phase), which is the reaction product of anatase-containing kaolinite (Range and Weiss, 1969), the only features are small, broad peaks at ~0.45 and 0.32 nm (19.7 and 27.8° 2θ).

Prior to the second heating at 900°C (Step 4), which was performed on a pressed pellet of the rinsed material to facilitate solid-state reaction, we observed that uni-

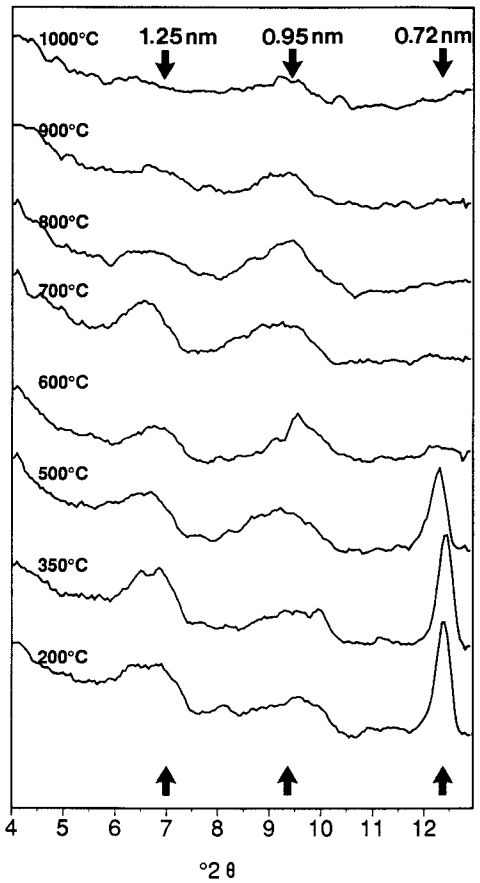

Figure 2. XRD profile (CuKα 4–13° 2θ) of kaolinite:NaCl heated for ~20 min at 200°, 350°, 500°, 600°, 700°, 800°, 900°, and 1000°C. Note that the 1.25 and 0.95 nm kaolinite:NaCl intercalate peaks persist well above the dehydroxylation temperature of kaolinite (500°–600°C).

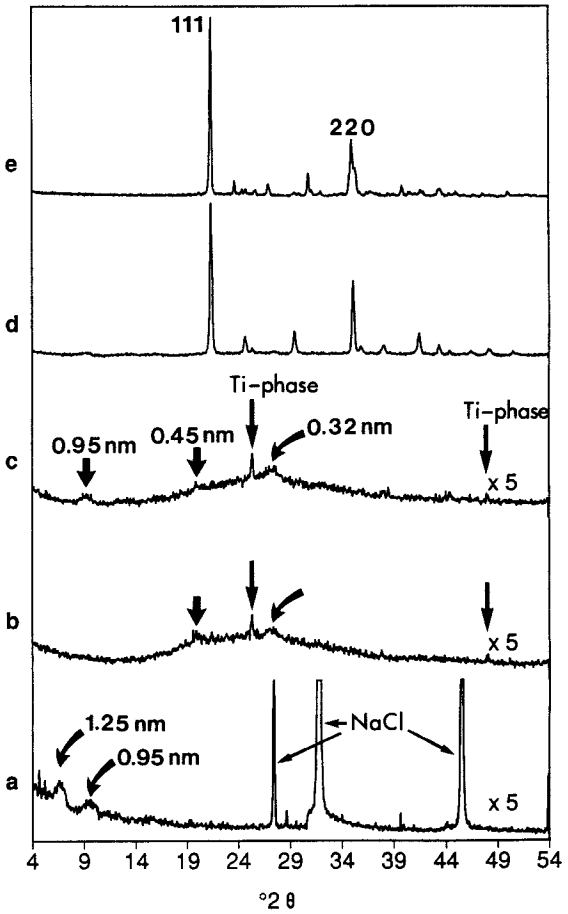

Figure 3. XRD profile (CuKα 4–54° 2θ) of (a) kaolinite:NaCl intercalate heated to 800°C for 40 min (Step 2), (b) rinsed 5 times and dried at 105°C overnight (Step 3), (c) uniaxially pressed, (d) then reheated at 900°C for 16 hours (Step 4). The XRD profile of synthetic low-carnegieite (e) is included for comparison. The vertical scale for (c), (d), and (e) is ×5 with respect to (a) and (b).

axial pressing caused the emergence of a broad peak at 0.95 nm (9.3° 2θ) and the reduction of the 0.45 nm peak relative to unpressed material, suggesting that these were basal and non-basal reflections, respectively (Figure 3c).

Heating the pressed pellet to 800°C caused no change in the profile, but when heated overnight (16 hours) at 900°C the XRD profile (Figure 3d) showed the disappearance of the broad hump and a set of sharp, intense reflections very similar to those of synthetic low-carnegieite ($NaAlSiO_4$) (shown in Figure 3e for comparison). Hereafter we refer to this phase as 'carnegieite.' The strong reflections corresponding to the 111 and 220 high-carnegieite reflections are indicated (Figure 3e). The weaker reflections in the two profiles (Figures 3d and 3e) are in poor agreement because they probably belong to other phases. In the Step 4 product profile there remain weak reflections due to the trace of $Al_4Ti_2SiO_{12}$ and a remnant of the 0.95 nm peak. Heating for a longer time or at a higher temperature resulted in the disappearance of the 'carnegieite' and the formation of the thermodynamically stable form of $NaAlSiO_4$ with the nepheline structure.

Solid-state NMR

Solid-state NMR is a powerful probe of local atomic structure in aluminosilicates (Kirkpatrick, 1988; Klinowski, 1988). The isotropic chemical shift is the most often exploited parameter in NMR as it is sensitive to local covalently bonded structure and to short range order in these structures.

^{29}Si NMR chemical shifts of tetrahedral silicon atoms in aluminosilicates have been shown to decrease from ~ −60 ppm to −115 ppm in passing from the Q^0 to Q^4 structures (Lippmaa *et al.*, 1980). In addition substitution of Al for nearest neighbour Si in an isostructural series increases the chemical shift by 5–6 ppm (Lippmaa *et al.*, 1981). For example, for Q^4 frame-

work silicon atoms the chemical shift of Si(0Al) lies in the range −100 to −110 ppm, while that for Si(1Al) lies in the range −95 to −105 ppm, and so on. Additional perturbations of the chemical shifts are provided by variations in the composition of the next nearest neighbour sites (Fyfe *et al.*, 1984), and distortions of bond angles and bond lengths (Thomas *et al.*, 1982; Higgins and Woessner, 1982). As a consequence of the sensitivity of the ^{29}Si chemical shift to composition the technique of ^{29}Si NMR has become an accepted method for determining Si/Al ratios and connectivities.

^{27}Al NMR shows less sensitivity to local structure than ^{29}Si NMR. For example, there exist 5 possible Si(nAl) environments for Q^4 Si but Loewenstein's rule limits the possible structures for Q^4 Al to one, i.e., Al(4Si). On the other hand, ^{27} Al NMR has been shown to be sensitive to the coordination state of the Al; tetrahedrally coordinated Al falls in the region 50 to 80 ppm, while octahedrally coordinated Al lies between 0 and 22 ppm. It is therefore possible to determine the ratio of framework to non-framework Al from the ^{27}Al spectra. However, the shape of ^{27}Al signals is often complicated by second order quadrupolar effects which are not removed by magic-angle spinning (MAS) (e.g., Kirkpatrick, 1988; Kohn *et al.*, 1989).

^{23}Na NMR of solids has been rarely studied. This is principally due to the large second order quadrupolar broadening of the central transition and the difficulty in separating chemical shift and quadrupolar effects. However, ^{23}Na MAS NMR has been used to study aluminosilicate glasses (Oestrike *et al.*, 1987; Kohn *et al.*, 1989) and feldspars and plagioclases (Kirkpatrick *et al.*, 1985; Yang *et al.*, 1986), while Kirkpatrick (1988) has reviewed the use of ^{23}Na MAS NMR in studies of minerals and glasses.

The ^{29}Si CP/MAS NMR spectrum (Figure 4a) of well-crystallized KGa-1 is identical to that reported by Barron *et al.* (1983). The splitting has been ascribed to either crystallographic inequivalence of Si sites (Barron *et al.*, 1983) or variations in hydrogen bonding (Thompson and Barron, 1987). The mean chemical shift of −91.1 ppm is consistent with a Q^3 environment for Si in kaolinite. The ^{29}Si CP/MAS NMR spectrum (Figure 4b) of the material after Step 1 appears identical to that of the original starting material (Figure 4a) but is probably dominated by the residual ~5% of unintercalated material in this specimen. Nevertheless, from the absence of other features we can conclude that the chemical environment of Si remains unchanged following intercalation, unlike in the various kaolinite: organic intercalates studied previously (Thompson, 1985) where the twin peaks disappeared and the signal was shifted to a higher field.

The ^{27}Al MAS NMR spectrum (Figure 5a) of well-crystallized KGa-1 shows a single asymmetric peak at −4.3 ppm (FWHM = 1300 Hz) due to the central +1/2 ↔ −1/2 transition, and a series of equally spaced spinning side bands on either side of the central peak which are assignable to the higher order transitions. The presence of well defined spinning side bands indicates the Al atoms are in a symmetrical environment. The spectrum is similar to that reported by Rocha and Klinowski (1990), Lambert *et al.* (1989), and Sanz *et al.* (1988), and indicates that the Al sites have octahedral symmetry. After treating KGa-1 with NaCl (Step 1) the ^{27}Al spectrum is unchanged (Figure 5b), indicating that there is no change in the kaolinite structure at this stage, in agreement with the ^{29}Si CP/MAS results. The

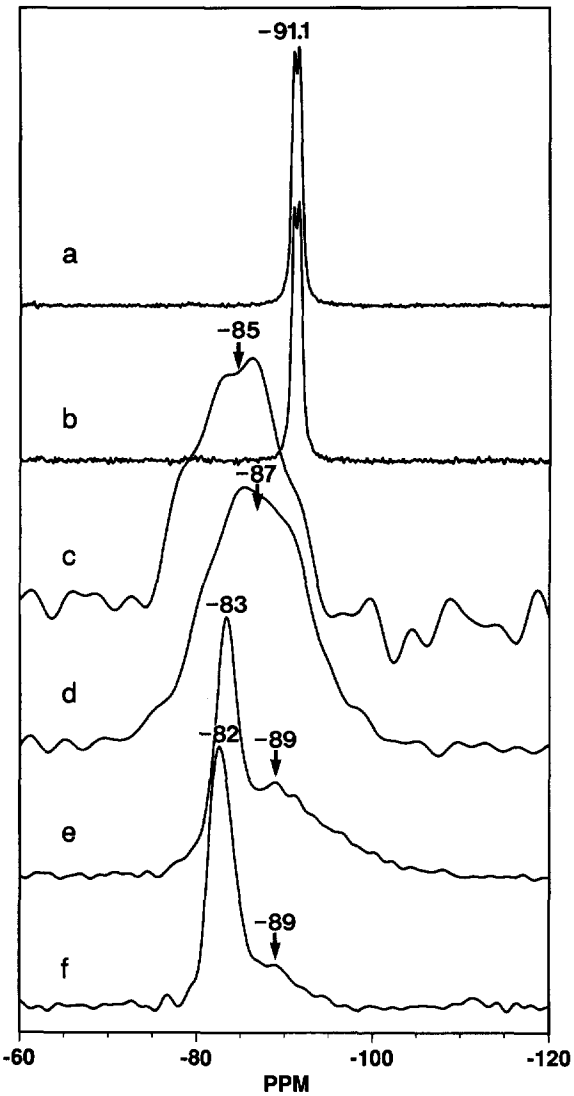

Figure 4. ^{29}Si NMR spectra of (a) kaolinite KGa-1, (b) kaolinite:NaCl after Step 1, (c) the intercalate heated to 800°C for 40 min (Step 2), (d) rinsed 5 times and dried at 105°C overnight (Step 3), (e) then reheated at 900°C for 16 hours (Step 4). The ^{29}Si NMR spectrum of synthetic low-carnegieite (f) is included for comparison.

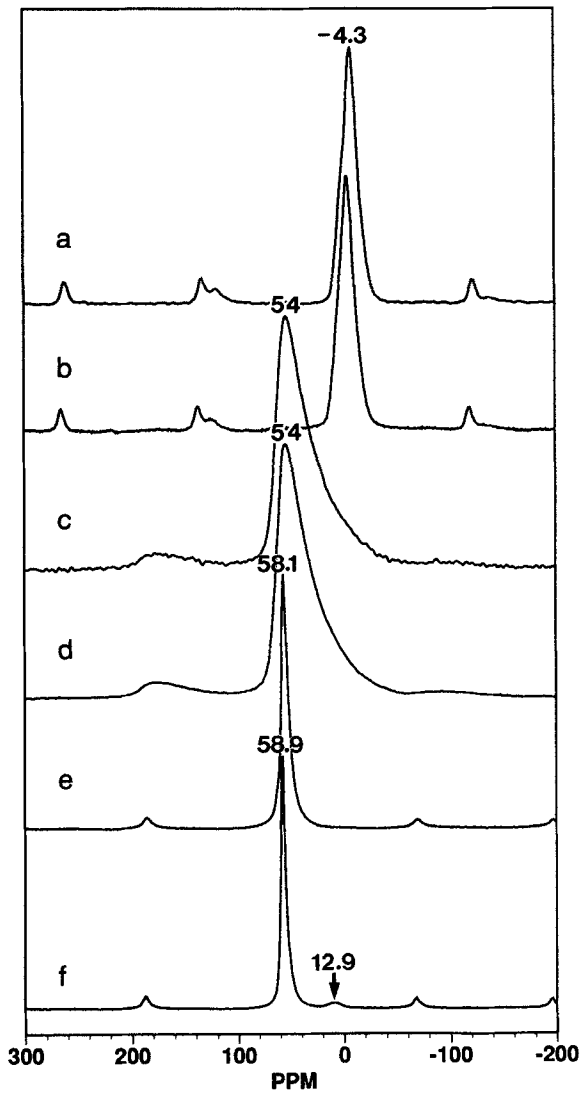

Figure 5. ^{27}Al NMR spectra of (a) kaolinite KGa-1, (b) kaolinite:NaCl after Step 1, (c) the intercalate heated to 800°C for 40 min (Step 2), (d) rinsed 5 times and dried at 105°C overnight (Step 3), (e) then reheated at 900°C for 16 hours (Step 4). The ^{27}Al NMR spectrum of synthetic low-carnegieite (f) is included for comparison.

^{23}Na NMR signal was clearly dominated by the narrow signal due to excess NaCl, namely regular octahedrally coordinated Na, and is not shown.

After the first heating (Step 2) the ^{29}Si CP/MAS NMR spectrum (Figure 4c) contains a broad featureless peak with a full width at half maximum (FWHM) of 850 Hz (15 ppm) and centred on −85 ppm. The signal-to-noise ratio of the spectrum was reduced dramatically, c.f. the product after Step 1 (Figure 4b). This may be due to (1) the dilution of the reaction product with NaCl; (2) the large increase in linewidth; or (3) a reduction in the cross-polarisation efficiency due to elimination of hydroxyl groups. In contrast, the ^{29}Si spectra for thermally treated kaolinite (metakaolinite) give broad, complex signals at progressively higher field with increasing temperature, −100 ppm at 650°C and −109 ppm at ~1000°C (Meinhold *et al.*, 1985). These results were later reproduced by Sanz *et al.* (1988), Lambert *et al.* (1989) and Rocha and Klinowski (1990). It is notable that 1:1 Na zeolite-A gives a single ^{29}Si resonance at −89 ppm; whereas, albite gives three resonances at −92, −96, and −104 ppm (Lippmaa *et al.*, 1980), and the Na containing zeolites, sodalite, and thomsonite give −84.8 and −83.5 ppm, respectively (Lippmaa *et al.*, 1981). The ^{27}Al NMR spectrum of the product (Figure 5c) gives a broad asymmetric signal (FWHM = 2700 Hz) at 54 ppm. The highly asymmetric nature of the peak is due to second order quadrupolar broadening, and is similar to that observed for albite by Kohn *et al.* (1989), and does not necessarily support the presence of AlO_5 and AlO_6. The structure typical for second order quadrupolar broadening is not observed on this peak, presumably because of the presence of a distribution of quadrupolar coupling constants. Furthermore, only the first spinning side bands are observable, suggesting a lower degree of symmetry at the Al sites. As after Step 1, the ^{23}Na NMR spectrum is still overwhelmed by the signal due to excess NaCl.

The ^{29}Si CP/MAS NMR of the rinsed material (Figure 4d), apart from a small shift to higher field to −87 ppm, is almost identical to that before rinsing, suggesting that rinsing has not significantly perturbed the short-range ordering even though it has thoroughly perturbed the long-range ordering. The same applies to the ^{27}Al NMR spectrum (Figure 5d). It is notable that the signal-to-noise in the ^{29}Si CP/MAS NMR spectrum is much improved because there is now no excess NaCl diluting the sample. It is also possible that the material has partly rehydrated upon rinsing, either through reaction with the inner surface or through incorporation of interlayer water molecules. Most striking of the NMR results is the ^{23}Na spectrum of this material (Figure 6a), which gives a single asymmetric peak at −21 ppm (FWHM = 3400 Hz). This peak position is typical of Na in aluminosilicates (Yang *et al.*, 1986; Kirkpatrick *et al.*, 1985; Oestrike *et al.*, 1987). No structure can be seen on the peaks indicating that the lineshape is dominated by a quadrupolar broadening, with a distribution of quadrupolar coupling constants or isotropic chemical shifts (Yang *et al.*, 1986; Krämer *et al.*, 1973). Comparison of the spectra with those in these references, and with those of Kohn *et al.* (1989) for albite suggest that the Na atoms are in an asymmetric environment.

The ^{29}Si NMR spectrum (Figure 4e) after Step 4 shows a well-defined peak at −83 ppm and a broad shoulder trailing off to high field to ~110 ppm, a marked change from the very broad signal centred on ~−87

ppm after Step 3. There is some evidence for a resolved peak in the shoulder at −89 ppm. We interpret these results by reference to the extensive ^{29}Si NMR studies (Lippmaa *et al.*, 1981; Fyfe *et al.*, 1984) on zeolites, in which a clear chemical shift resolution of Si(nAl), $0 \leq n \leq 4$, is observed for that family of framework aluminosilicates. Carnegieite, as a 'stuffed' cristobalite (O'Keeffe and Hyde, 1976), is also a framework aluminosilicate and would be expected to show similar chemical shift resolution of Si(nAl) environments. In high-carnegieite there is only one Si site and one Al site which possess Si(4Al) and Al(4Si) connectivities, respectively (Barth and Posnjak, 1932). Despite the lower symmetry of low-carnegieite, we assign the signal at about −82 ppm to Si(4Al). By analogy with Na-zeolites, the substitution of Al by Si shifts the signal ~6 ppm to higher field with each successive substitution (Bennett *et al.*, 1983; Newsam, 1985). Therefore, the small signal at ~−89 ppm in the low-carnegieite specimen is attributed to the presence of some Si(3Al), implying imperfect Si-Al ordering in the structure. The Step 4 product is also dominated by Si(4Al) but a large proportion (>30%) of Si(3Al) is also present, as well as progressively lesser quantities of Si(2Al) and Si(1Al). There is no Si(0Al) ordering, i.e., cristobalite-like, present. The ^{27}Al spectrum (Figure 5e) has a single narrow peak (FWHM = 500 Hz) at 58.1 ppm indicating tetrahedral symmetry. This compares with synthetic low-carnegieite (Figure 5f) which has a narrow peak at 58.9 ppm (FWHM = 350 Hz) due to tetrahedral Al, and a slightly broader peak (FWHM = 1200 Hz) at 12.9 ppm due to octahedral Al. The estimated ratio of tetrahedral to octahedral Al is 22:1. It should be noted that perfectly ordered carnegieite should not have either Si(3Al) connectivity or AlO_6 coordination, but the as synthesized material (Klingenberg *et al.*, 1981) has small amounts of both. The ^{23}Na spectrum of Step 4 product (Figure 6b) is more anisotropic than for the rinsed material, and there may be an inflection at −30 ppm indicative of second order quadrupolar coupling (c.f., the spectra of Yang *et al.*, 1986). The long tail of these spectra is consistent with the distribution of quadrupolar coupling tensors, and less so to a distribution of isotropic chemical shifts (M. E. Smith, personal communication). Separation of these effects would be facilitated by measurement at several field strengths (Kohn *et al.*, 1989; Sato *et al.*, 1991). The spectrum after step 4 is similar to that of synthetic carnegieite (Figure 6c).

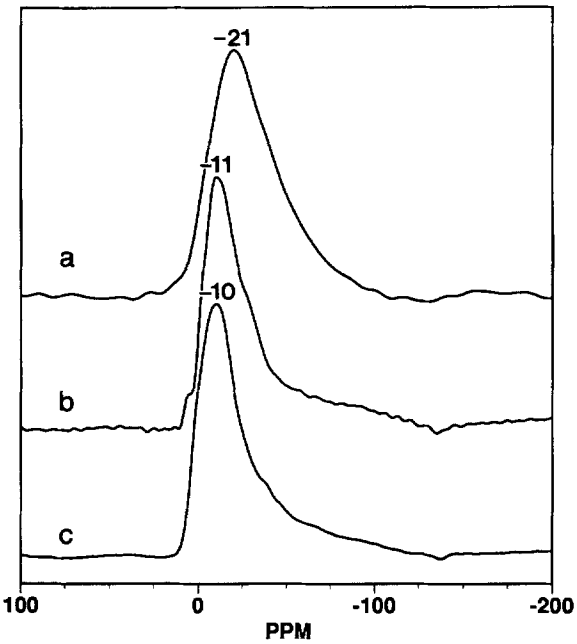

Figure 6. ^{23}Na NMR of (a) kaolinite:NaCl intercalate heated to 800°C for 40 min then rinsed 5 times and dried at 105°C overnight (Step 3), (b) then reheated at 900°C for 16 hours (Step 4). The ^{23}Na NMR spectrum of synthetic low-carnegieite (c) is included for comparison.

FTIR

The FTIR spectrum of the intercalate (Figure 7b) is almost the same as that of kaolinite (Figure 7a) except that there is some additional molecular water present in the intercalate (broad band centered on ~3400 cm^{-1}) and the structure within 1000–1150 cm^{-1} band due to Si-O stretching modes is better resolved. It is probable that the ~5% unintercalated kaolinite dominates this spectrum. After Step 2 the FTIR spectrum (Figure 7c) is now quite different. Nearly all the hydroxyl modes have disappeared but a small quantity of molecular water persists. The fine structure in the 1000–1150 cm^{-1} band due to Si-O stretching modes blurs out into a broader band with a large shoulder (much larger than metakaolinite) out to 1500 cm^{-1}. The Al-O-H bending modes at 910 and 940 cm^{-1} disappear. A strong band at ~700 cm^{-1} is enhanced unlike in metakaolinite where a similar band emerges at ~800 cm^{-1} (Percival *et al.*, 1974; Rocha and Klinowski, 1990). There appears to be little structural change following rinsing (Figure 7d). While it was hoped to observe the above-postulated increase in the molecular water present in this specimen upon rinsing, the FTIR spectrum was not helpful as a quantitative check, probably due to adsorbed water.

The FTIR spectra of the material after Step 4 and synthetic low-carnegieite are presented in Figure 7e and 7f, respectively. Both spectra show the same general features: a broad 'Si-O' stretching mode at 990 cm^{-1} with an extended shoulder to high wavenumber, a sharper band at 690 cm^{-1}, and negligible molecular water (probably adsorbed). Surprisingly these spectra are identical to that of the rinsed material (Figure 7d) except for the molecular water.

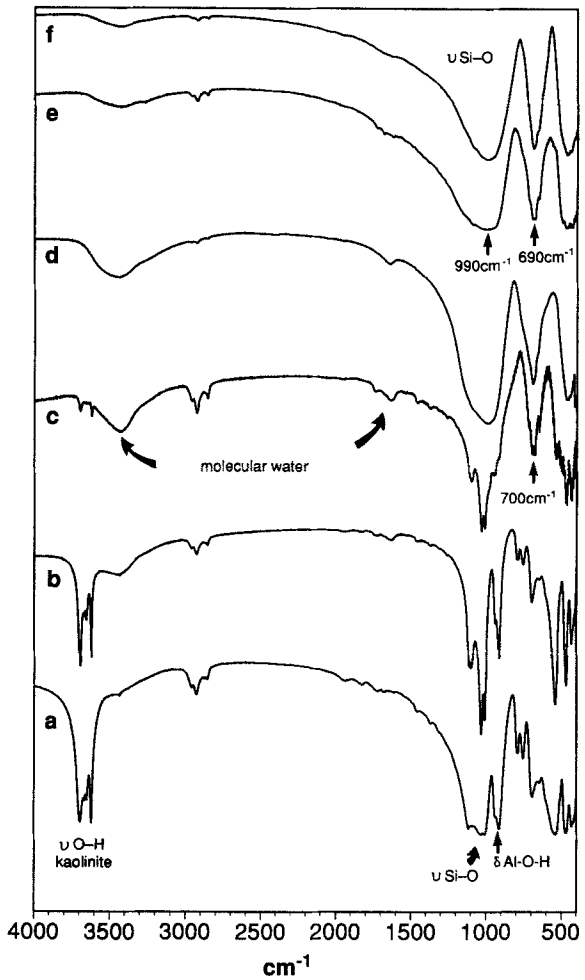

Figure 7. FTIR spectra (4000–400 cm^{-1} at 1 cm^{-1} resolution) of (a) kaolinite KGa-1, (b) kaolinite:NaCl intercalate (Step 1), (c) Kaolinite:NaCl intercalate heated to 800°C for 40 min (Step 2), (d) rinsed 5 times and dried at 105°C overnight (Step 3), (e) then reheated at 900°C for 16 hours (Step 4). The corresponding FTIR spectrum of synthetic low-carnegieite (f) is included for comparison.

Microscopy

Scanning electron micrographs of the starting material, KGa-1 well-crystallized, the reaction products of Steps 1 to 4, and the synthetic low-carnegieite are shown in Figures 8a–f, respectively. What is most striking about this sequence is the extent to which the external morphology of the individual kaolinite crystals as well as the characteristic book-like aggregation of crystals are preserved through the reaction sequence.

The kaolinite:NaCl intercalate, Figure 8b, is identical in appearance to the starting kaolinite (Figure 8a). After heating at 800°C for 40 minutes, despite having undergone relatively rapid dehydroxylation, the crystals still retain their external morphology. Figure 8c shows that these intercalate crystals have a distinctive powdery coating which is probably the excess NaCl still present in the material. After rinsing with distilled water then drying at 105°C, the morphology is still preserved (Figure 8d). Following the second heating at 900°C (Step 4), there is a noticeable change, but there are still indications of the original kaolinite morphology (Figure 8e). This contrasts with the appearance of the synthetic low-carnegieite which displays a quite different form (Figure 8f).

Semi-quantitative energy-dispersive X-ray analysis (EDS) was performed on the reaction products of Steps 3 and 4. Due to the vast excess of NaCl present in the reaction products of Steps 1 and 2 it was not feasible to perform the same analysis on these specimens.

Transmission electron microscopy confirmed that the hexagonal platey morphology of the kaolinite crystals is fully preserved in Steps 1 through 3. Unfortunately, very rapid damage by the electron beam precluded the recording of lattice images of the 0.95 and 1.25 nm layer repeats for these or any of the intercalated specimens.

DISCUSSION

Step 1. Initial reaction with NaCl (intercalation step)

We interpret the observation of two basal dimensions, 1.25 nm and 0.95 nm, as indicating two intercalates with differing thickness of the NaCl filling. Weiss *et al.* (1966) reported 1.013 nm for material prepared by entrainment via ammonium acetate. These two intercalates are represented schematically in Figures 9b and 9c with respect to the starting kaolinite (Figure 9a). That Na is adjacent to the tetrahedral silicate sheet and Cl adjacent to the hydroxyls is required by the polarisation of the kaolinite structure.

Step 2. Heating the intercalate

The persistence of the peaks at 1.25 nm and 0.95 nm suggests that the layered nature of the intercalate is preserved. This is consistent with SEM and TEM observations on this material (Figure 8c) which still show no alteration in crystal morphology. The absence of a metakaolinite-like broad 'hump' between 0.45 and 0.30 nm (i.e., 19 and 30° 2θ) is striking. The FTIR data and the disappearance of octahedrally coordinated Al in favour of tetrahedrally coordinated Al require that the intercalate has undergone dehydroxylation, but in a manner quite unlike metakaolinite. It would appear that chemical reaction occurs within the intercalate with a minimum of transport and maximum retention of structural framework.

$$Al_2Si_2O_5(OH)_4 + 2NaCl \rightarrow 2NaAlSiO_4 + 2HCl + H_2O. \quad (1)$$

Now both the Si and Al are in tetrahedral coordination and the MO_4 tetrahedra have condensed together in such a way that the local chemical environment is more like a zeolite than a feldspar (from the perspective of

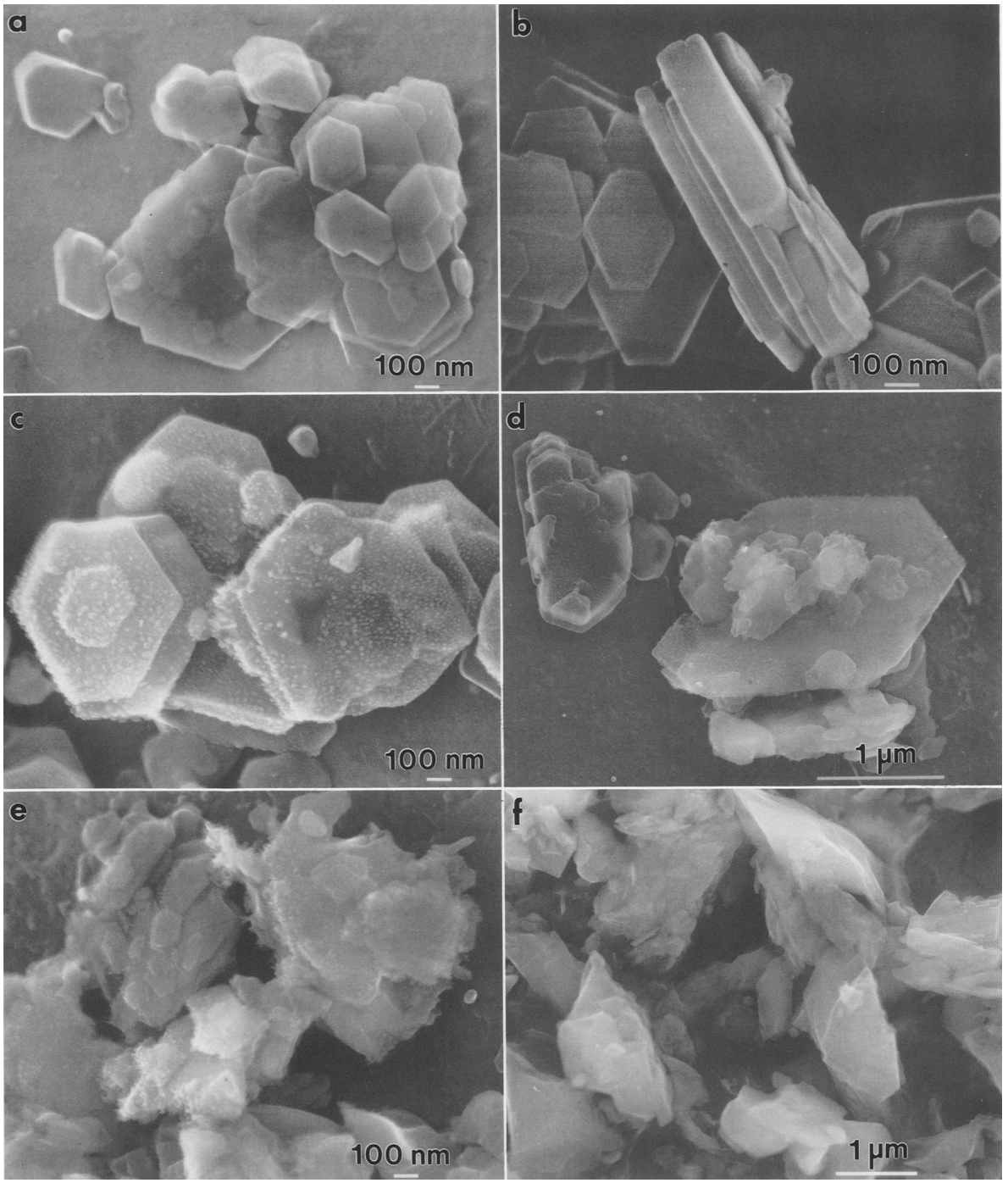

Figure 8. Scanning electron micrographs (secondary electron images) of (a) kaolinite KGa-1, (b) kaolinite:NaCl after Step 1, (c) the intercalate heated to 800°C for 40 min (Step 2), (d) rinsed 5 times and dried at 105°C overnight (Step 3), (e) then reheated at 900°C for 16 hours (Step 4). The scanning micrograph for synthetic low-carnegieite (f) is included for comparison with (e).

the Si, at least). Figure 9d shows a schematic representation of the reaction product after Step 2 which would be consistent with the observed XRD and spectroscopic data.

The linewidth of the ^{29}Si NMR signal after Step 2 is significant. With respect to zeolites, the contributions to ^{29}Si NMR linewidths have been thoroughly investigated (Fyfe *et al.*, 1984). One major contributor is

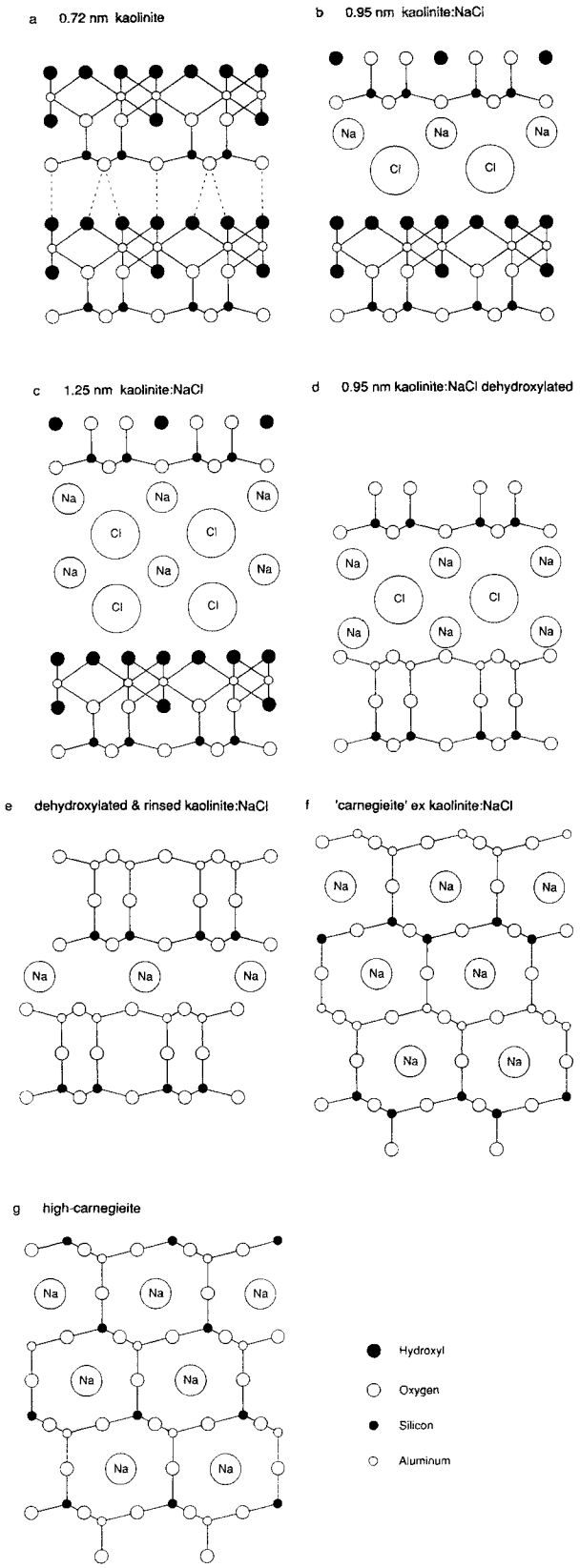

crystallographic inequivalence of sites, either as a result of imperfect Si-Al ordering in a well-crystallized material or in a structurally disordered or amorphous material. Another major contributor is the line-broadening effect of ^{27}Al in an asymmetric environment. The XRD data for Step 2 product suggest that both causes would be involved in generating the broad signal in Figure 4c. The Step 2 product is almost certainly a layered material and would, therefore, more closely resemble kaolinite than a zeolite. Taking into account the difficulty in interpreting the ^{29}Si chemical shifts derived from such broad signals, we propose that the connectivity implied by Figure 9d [i.e., Si(1Al)], is probably still consistent with the observed ^{29}Si NMR data. Interpreting the chemical shift of −85 ppm in terms of zeolite connectivity would imply Si(3Al) (Lippmaa *et al.*, 1981). However, interpreting it in terms of the ^{29}Si signal for kaolinite, the broadened signal has only shifted downfield by 6 ppm after Step 2.

Step 3. Rinsing to remove excess NaCl and drying

Rinsing the thermally treated intercalate clearly destroys long-range order and gives the XRD profile a metakaolinite-like appearance. However, both the solid-state NMR and FTIR spectroscopic evidence require that its structure be quite unrelated. A proposed structural model of the material after Step 3 is presented as Figure 9e. Partial rehydration of the structure was suspected also, but there was no evidence of well-resolved hydroxyl stretching modes in the FTIR. SEM of this material once again suggests an overall preservation of the external morphology (Figure 8d). The X-ray spectrum of this material was consistent with the expected stoichiometry as presented in Eq. (1) above, namely, $NaAlSiO_4$. We detected a trace of Cl, however, suggesting that the rinsing was not yet complete. A small amount of Ti was also observed, consistent with the observation of $Al_4Ti_2SiO_{12}$ in the XRD profile.

Step 4. Second heating at 900°C

The absence of sodalite and the appearance of the carnegieite-related material confirm the plausibility of the reaction at Step 2 as given in Eq. (1). That pressing the rinsed material (Figure 3c) appeared to reconstitute the 0.95 nm layering indicates that this is the true layer repeat when there is no excess NaCl about.

The X-ray spectrum of this material was identical

←

Figure 9. Schematic representation of (a) kaolinite, (b) kaolinite:NaCl 0.95 nm intercalate (Step 1), (c) kaolinite:NaCl 1.25 nm intercalate (Step 1), (d) kaolinite:NaCl 0.95 nm intercalate heated to 800°C (Step 2), (e) Step 2 product rinsed and dried (Step 3), and finally (f) 'carnegieite' formed by heating Step 3 product at 900°C (Step 4). A [110] projection of the structure of ideal high-carnegieite is schematically presented in (g).

to that of the Step 3 reaction product except that the Cl had disappeared. Presumably the Cl in the Step 3 product had reacted with the remnant water to given off as HCl. Otherwise the chemical composition was preserved through Step 4.

What is most interesting about the reaction of the rinsed material to form a carnegieite-related product is the temperature at which this occurs. The stable polymorph of $NaAlSiO_4$ at 1 atm and from room temperature to 1250°C has the nepheline structure. Above that to the solidus it has the carnegieite ('stuffed' cristobalite) structure. In other words, Step 4 produces well-crystallized 'carnegieite' at temperatures well below its apparent thermodynamic stability field. This can be understood if we invoke a mechanism which is kinetically favourable to the formation of 'carnegieite-type' and unfavourable to the formation of 'nepheline-type.' In Figure 9f we have presented a schematic model of 'carnegieite' formed from Step 4. This is compared with a [110] projection of high-carnegieite in Figure 9g.

Assuming that the schematic model of the rinsed material (shown in Figure 9e) is plausible, all that is required to transform this material to 'carnegieite' is a minor rearrangement of part of the structure which involves the inversion of alternate MO_4 tetrahedra. The only difference between this 'carnegieite' and high-carnegieite, therefore, is the Si-Al ordering. This proposed topotactic mechanism, which would be kinetically favourable, is only partly consistent with the NMR data. The Si-Al ordering implied by this topotactic model would give pure Si(1Al). The observed ^{29}Si spectrum (Figure 4e) suggests that the 'carnegieite' structure cannot accommodate such segregation. On the other hand it does show that the Step 4 product is quite short of high-carnegieite, i.e., Si(4Al), ordering. The Si-Al ordering of this product has stopped somewhere in between pure Si(1Al) and pure Si(4Al). High-carnegieite (Smith and Tuttle, 1957) undergoes a phase transition at 690°C (Klingenberg *et al.*, 1981) to a much lower symmetry low-temperature polymorph as represented by Figure 3d, though the lower symmetry results from distortion of the ideal cubic framework rather than any rearrangement of Si and Al. While the Step 4 produced material cannot be readily indexed to a unique unit cell, the general similarity between the XRD, NMR and FTIR data for the synthetic carnegieite and the Step 4 product leads us to conclude that the Step 4 product is structurally closely related to low-carnegieite.

CONCLUSIONS

The formation of kaolinite:NaCl intercalate without the use of an entraining agent is of particular interest because the intercalation process is relatively facile and the starting materials, namely kaolinite, halite, and water, are abundant and inexpensive. The subsequent heating and rinsing steps produce several previously unreported materials:

1) the dehydroxylated kaolinite:NaCl intercalate which retains its layered structure;
2) the dehydroxylated, rinsed material which is chloride-free and shows no long-range order, yet necessarily also retains a layered structure. This material is very chemically reactive and is likely to have unusual physical properties;
3) the carnegieite-like material which is formed at 350°C below the carnegieite stability field.

The sequence of reaction steps described in this investigation on the kaolinite:NaCl intercalate are almost certainly applicable to all alkali halides. In addition to providing a very reactive form of homogenous alkali aluminosilicate following Step 3, it will also provide a novel synthetic route to the formation of low-temperature crystalline polymorphs of $MAlSiO_4$, M = alkali. These further investigations are now in progress.

ACKNOWLEDGMENTS

The authors wish to thank Dr. M. E. Smith for advice on the interpretation of the NMR spectra and Mr. Dénes Bogsányi for collecting the FTIR spectra. Mr. Neil Gabbitas provided invaluable assistance in preparation of the NMR figures. This work has been supported by an ARC Small Grant.

REFERENCES

Barron, P. F., Frost, R. L., Skjemstad, J. O., and Koppi, A. (1983) Detection of two silicon environments in kaolins via solid state ^{29}Si NMR: *Nature* **302,** 49–50.

Barth, T. F. W., and Posnjak, E. (1932) Silicate structures of the cristobalite type: I. The crystal structure of α-cristobalite ($NaAlSiO_4$): *Z. Kristallogr.* **81,** 135–141.

Bennett, J. M., Blackwell, C. S., and Cox, D. E. (1983) High-resolution silicon-29 nuclear magnetic resonance and neutron powder diffraction study of Na-A zeolite. Loewenstein's rule vindicated: *J. Phys. Chem.* **87,** 3783–3790.

Calvert, C. S. (1984) Simplified, complete CsCl-hydrazine-dimethylsulfoxide intercalation of kaolinite: *Clays & Clay Minerals* **32,** 125–130.

Deer, W. A., Howie, R. A., and Zussman, J. (1966) *An Introduction to the Rock-forming Minerals:* Longman, London, 375 pp.

Fyfe, C. A., Gobbi, G. C., Murphy, W. J., Ozubko, R. S., and Slack, D. A. (1984) Investigation of the contributions to the ^{29}Si MAS NMR line widths of zeolites and the detection of crystallographically inequivalent sites by the study of highly siliceous zeolites: *J. Am. Chem. Soc.* **106,** 4435–4438.

Gábor, M., Pöppl, L., Izvekov, V., and Beyer, H. (1989) Interaction of kaolinite with organic and inorganic alkali metal salts at 25–1300°C: *Thermochim. Acta* **148,** 431–438.

Higgins, J. B., and Woessner, D. E. (1982) ^{29}Si, ^{27}Al and ^{23}Na NMR spectra of framework silicates: *EOS, Trans. Am. Geophys. Union* **63,** p. 1139.

Jackson, M. L. and Abdel-Kader, F. H. (1978) Kaolinite intercalation procedure for all sizes and types with X-ray

spacing distinctive from other phyllosilicates: *Clays & Clay Minerals* **17,** 157–167.

Kirkpatrick, R. J. (1988) MAS NMR spectroscopy of minerals and glasses: in *Spectroscopic Methods in Mineralogy and Geology,* F. C. Hawthorne, ed., Reviews in Mineralogy **18,** Mineralogical Society of America, Washington, 341–403.

Kirkpatrick, R. J., Kinsey, R. A., Smith, K. A., Henderson, D. M., and Oldfield, E. (1985) High resolution solid-state sodium-23, aluminum-27, and silicon-29 nuclear magnetic resonance spectroscopic reconnaissance of alkali and plagioclase feldspars: *Amer. Miner.* **70,** 106–123.

Klingenberg, R., Felsche, J., and Miehe, G. (1981) Crystal data for the low-temperature form of carnegieite $NaAlSiO_4$: *J. Appl. Crystallogr.* **14,** 66–68.

Klinowski, J. (1988) Recent advances in solid-state NMR of zeolites: *Annu. Rev. Mater. Sci.* **18,** 189–218.

Kohn, S. C., Dupree, R., and Smith, M. E. (1989) A multinuclear magnetic resonance study of the structure of hydrous albite glasses: *Geochim. Cosmochim. Acta* **53,** 2925–2935.

Krämer, F., Müller-Warmuth, W., Scheerer, J., and Dutz, H. (1973) Sodium-23 and lithium-7 NMR studies of silicate and borate glasses: *Z. Naturforsch. Tiel A* **28,** 1338–1350.

Lambert, J. F., Millman, W. S., and Fripiat, J. J. (1989) Revisiting kaolinite dehydroxylation: A ^{29}Si and ^{27}Al MAS NMR study: *J. Am. Chem. Soc.* **111,** 3517–3522.

Lippmaa, E., Mägi, M., Samoson, A., Engelhardt, G., and Grimmer, A.-R. (1980) Structural studies of silicates by solid-state high-resolution ^{29}Si NMR: *J. Am. Chem. Soc.* **102,** 4889–4893.

Lippmaa, E., Mägi, M., Samoson, A., Tarmak, M., and Engelhardt, G. (1981) Investigation of the structure of zeolites by solid-state high-resolution ^{29}Si NMR spectroscopy: *J. Am. Chem. Soc.* **103,** 4992–4996.

Meinhold, R. H., MacKenzie, K. J. D., and Brown, I. W. M. (1985) Thermal reactions of kaolinite studied by solid state ^{27}Al and ^{29}Si NMR: *J. Mater. Sci. Lett.* **4,** 163–166.

Miller, J. G., and Oulton, T. D. (1972) Prototropy in kaolinite during percussive grinding: *Clays & Clay Minerals* **18,** 313–323.

Newsam, J. M. (1985) The influence of second-neighbour aluminums on the isotropic chemical shift of ^{29}Si in a zeolite environment: *J. Phys. Chem.* **89,** 2002–2005.

Oestrike, R., Yang, W. H., Kirkpatrick, R. J., Hervig, R. L., Navrotsky, A., and Montez, B. (1987) High-resolution ^{23}Na, ^{27}Al, and ^{29}Si NMR spectroscopy of framework aluminosilicate glasses: *Geochim. Cosmochim. Acta* **51,** 2199–2209.

O'Keeffe, M., and Hyde, B. G. (1976) Cristobalites and topologically-related structures: *Acta Crystallogr. Sect. B.* **32,** 2923–2936.

Percival, H. J., Duncan, J. F., and Foster, P. K. (1974) Interpretation of the kaolinite-mullite reaction sequence from infrared absorption spectra: *J. Am. Ceram. Soc.* **57,** 57–61.

Range, K. J. and Weiss, A. (1969) Titanium in the kaolinite lattice and formation of pseudoanatase during thermal dissociation of kaolins containing titanium: *Ber. Dtsch. Keram. Ges.* **46,** 629–634.

Rocha, J., and Klinowski, J. (1990) ^{29}Si and ^{27}Al magic-angle-spinning NMR studies of the thermal transformation of kaolinite: *Phys. Chem. Miner.* **17,** 179–186.

Sanz, J., Madani, A., Serratosa, J. M., Moya, J. S., and Aza, S. (1988) Aluminium-27 and silicon-29 magic-angle spinning nuclear magnetic resonance study of the kaolinite-mullite transformation: *J. Am. Ceram. Soc.* **71,** C418–C421.

Sato, R. K., McMillan, P. F., Dennison, P., and Dupree, R. (1991) High-resolution ^{27}Al and ^{29}Si NMR investigation of SiO_2-Al_2O_3 glasses: *J. Phys. Chem.* **95,** 4483–4489.

Smith, J. V., and Tuttle, O. F. (1957) The nepheline-kalsilite system. I X-ray data for crystalline phases: *Am. J. Sci* **255,** 282–305.

Sugahara, Y., Satokawa, S., Kuroda, K., and Kato, C. (1988) Evidence for the formation of interlayer polyacrylonitrile in kaolinite: *Clays & Clay Minerals* **36,** 343–348.

Sugahara, Y., Satokawa, S., Kuroda, K., and Kato, C. (1990) Preparation of a kaolinite-polyacrylamide intercalation compound: *Clays & Clay Minerals* **38,** 137–143.

Thomas, J. M., Fyfe, C. A., Ramdas, S., Klinowski, J., and Gobbi, G. C. (1982) High-resolution silicon-29 nuclear magnetic resonance spectrum of zeolite ZK-4: Its significance in assessing magic-angle-spinning nuclear magnetic resonance as a structural tool for aluminosilicates: *J. Phys. Chem.* **86,** 3061–3064.

Thompson, J. G. (1985) Interpretation of solid state ^{13}C and ^{29}Si nuclear magnetic resonance spectra of kaolinite intercalates: *Clays & Clay Minerals* **33,** 173–180.

Thompson, J. G., and Barron, P. F. (1987) Further consideration of ^{29}Si NMR spectrum of kaolinite: *Clays & Clay Minerals* **35,** 38–42.

Thompson, J. G., and Cuff, C. (1985) Crystal structure of kaolinite: dimethylsulfoxide intercalate: *Clays & Clay Minerals* **33,** 490–500.

Weiss, A., Thielepape, W., and Orth, H. (1966) Neue Kaolinit-Einlagerungsverbindungen: in *Proc. Int. Clay Conf., Jerusalem, 1966, Vol. 1,* L. Heller and A. Weiss, eds., Israel Program for Scientific Translations, Jerusalem, 277–293.

Yang, W. H., Kirkpatrick, R. J., and Henderson, D. M. (1986) High-resolution ^{29}Si, ^{27}Al, and ^{23}Na NMR spectroscopic study of Al-Si disordering in annealed albite and oligoclase: *Amer. Mineral.* **71,** 712–726.

(Received 8 January 1992; accepted 12 May 1992; Ms. 2172)